Modelling the within-host growth of viral infections in insects: Electronic supplementary material

Steven M. White[1,2]*, John P. Burden[1], Philip K. Maini[2,3] and Rosemary S. Hails[1]

May 15, 2012

[1] Centre for Ecology & Hydrology, Maclean Building, Benson Lane, Crowmarsh Gifford, Wallingford, Oxfordshire, OX10 8BB, United Kingdom.

[2] Centre for Mathematical Biology, Mathematical Institute, University of Oxford, 24-29 St Giles', Oxford, Oxfordshire, OX1 3LB, United Kingdom.

[3] Oxford Centre for Integrative Systems Biology, Department of Biochemistry, South Parks Road, Oxford, OX1 3QU, United Kingdom.

*Email: smwhit@ceh.ac.uk

1 Insect and virus stocks

Spodoptera exigua larvae were obtained from Syngenta (Jeallotts Hill, UK) in 2003 and reared in continuous culture on artificial diet [1]. This population was shown to be free from persistent baculovirus infections by PCR and RT-PCR for the viral polyhedrin gene using total insect DNA as a template.

Four different baculoviruses were used in this study; the Oxford strain of *Mamestra brassicae* nucleopolyhedrovirus (*Mb*NPV) [2], *Panolis flammea* nucleopolyhedrovirus (*Pafl*NPV) variant 4 [3], *Autographa californica* nucleopolyhedrovirus (*Ac*NPV) strain C6 [4] and *Spodoptera exigua* nucleopolyhedrovirus (*Se*NPV) [5]. Stocks of each virus were made by dosing third instar *S. exigua* larvae with 10^8 occlusion bodies (OBs) by diet plug feeding [6], and purifying the virus by density gradient centrifugation [1]. The titre of the purified virus stock was estimated using an Improved Neubauer haemocytometer (B.S. 748, Weber, UK) and the virus stored at -20°C. Virus stocks were re-counted before each use.

2 Statistical Methods

The data were analysed using generalised linear modelling techniques (GLIM version 3.77, Royal Statistical Society, 1985). For the analysis of mortality all explanatory variables (virus concentration, virus, block) and their interactions were fitted to the mortality data. A binomial error structure was assumed, which was substantiated by subsequent inspection of the scale parameter [7]. The contribution of each term was tested for significance and non-significant terms removed to leave the minimal adequate model. Box-Cox transformations indicated an inverse transformation was required for data on time to larval death.

3 DNA Extraction & Quantification

DNA (insect and viral) was extracted from the frozen larvae by first thawing them and then disrupting them using a manual tissue grinder. Total DNA was then extracted from this material using a DNEasy mini kit (Qiagen). The DNA was eluted from the column into

200μl of elution buffer and quantified by spectrophotometry at 260nm and 280nm. Extracted DNA was stored at -20°C. DNA was extracted from 5 of the larvae harvested at each time point.

Viral DNA was quantified by real-time PCR using a Rotor Gene RG-3000 (Corbett Research) and a CAS-1200 liquid handling system (Corbett Research). Primer pairs were designed, specific to the sequence of each virus, to amplify a region of approximately 200 base pairs (bp) from the viral ie1 gene (*Ac*IE1-1 AAGGTGTGGTGGGCCAGTTT, *Ac*IE1-2 TGGTCGGAGAACCTGTTGGA, *Mb*IE1-1 TTGCTTCCGAAGGACCACAA, *Mb*IE1-2 ATCCCGTGTCGAGCAAATGA, *Pf*IE1-1 CGTCAACGGCATCAACAACA, *Pf*IE1-2 TGGCAGCTCCTTTTCCAACA, *Se*IE1-1 TCGACAACAGCGGCATCTTT, *Se*IE1-2 CGGTAGCGTTCGATGGTGAC).

Each real-time PCR reaction mixture consisted of Platinum SYBR Green qPCR SuperMix-UDG (Invitrogen) (10μl), sterile distilled water (6.2μl), BSA (1μl), and the appropriate primers (10pmol/μl, 0.4μl of each primer) to which was added 2μl of the extracted total DNA. The reaction profile was a single cycle of 50°C for 2 minutes, followed by 40 cycles of 95°C for 15 seconds, 57°C for 15 seconds and 72°C for 15 seconds. This was followed by a stage in which the temperature was raised from 57°C to 99°C in 1°C intervals to allow for subsequent melt curve analysis.

For each sample duplicate real-time PCR reactions were run and each PCR run included duplicate negative controls in which the template DNA was replaced by 2μl of sterile distilled water. For the quantification of the samples, genomic DNA from the appropriate virus was used to generate a standard curve. Viral genomic DNA was purified by caesium chloride gradient purification of DNA released from virus particles [6]. For each set of quantification reactions a series of five decimal dilutions of the viral genomic DNA was set up using the CAS-1200 system. This dilution series was made from an initial sample of the virus DNA which had been quantified by spectrophotometry at 260nm and 280nm. Standard samples were also run in duplicates. A standard curve was generated based on this dilution series using the software associated with the RG-3000, which also quantified the samples based on

this curve. Standard curves with an R2 value of less than 0.99 were rejected. Samples were only regarded as giving a positive real-time PCR result if the take-off point of the reaction was before that seen with any primer dimers produced in the negative control reactions and a product with the appropriate denaturation temperature was seen on the melt-curve analysis.

An average of two duplicates was taken to be the quantification for a given sample. As the total amount of DNA in the PCR reaction was known (2μl of known concentration in each reaction) the proportion of this which was viral could therefore be calculated.

4 Consequences of Censoring Technique

One drawback of our sampling method is that data points towards the end of the time series are censored. Some insects died before the final time point, so those censored at the final time point are selected from those that survived. There are likely to be yield differences depending upon time of death, and therefore the final sub-sample will be biased. It is unclear how this affects our results, but it is most likely to affect host-pathogen systems where one compares a virus with a high degree of variance in the speed of kill to a virus with a low degree of variance (which does not apply here) as this will influence the degree of bias. To combat this, the only solution would be to monitor the growth of virus in individual larvae by subsampling from the same insect throughout the course of infection. However, there are a number of technical issues with sampling tissue and accurately estimating total virus abundance within the host without killing the insect.

5 Virus Growth Rate

By equation (B.3), the model predicts that the initial growth rate is double exponential. This is faster than the single exponential growth rate that is common in many other infection models. Indeed, using an approximation to equation (B.3) such that

$$V(t) \approx V_0 \exp\{\beta_0 H_0 t\} \tag{1}$$

equation (1) underpredicts the growth of virus (see Figure S2).

6 Prescribing r_0

In the main text we show the results of the model fitting whereby all model parameters are fitted to the data from infected individuals simultaneously. This is done so that we account for stochastic differences between treatments and to allow the value to be and emergent property of the simultaneous fitting. However, r_0, the maximum host growth, is the innate parameter of host growth and should be independent of the infection. Hence, an alternative fitting strategy could be to fit r_0 from the initial control data (i.e. before any pupation effects occur), fix this parameter and fit the remaining parameters as described by the previous method. In this section, we carry out this fitting and discuss the implications.

The results of prescribing r_0 are shown in Table S1. Comparing this result to our previous result (Table 1 in the main text), we see that the biggest effect is on the host growth reduction rate, a. Here we see a large increase in this parameter value compared to the previous fitting. This difference would suggest that, by not fitting fixing the maximum host growth rate to the control data, the fitting method underestimates the host growth slow-down caused by the virus.

7 Dependence on the Speed of Kill

In Figures S3 and S4 we have further explored the impacts of the speed of kill on the host mass (left hand column) and yield (right hand column) for all 6 parameters (rows) in the model for two contrasting virus strains: *Ac*NPV and *Se*NPV. The results are discussed in the main text Discussion.

References

[1] F. R. Hunter-Fujita, P. F. Entwistle, H. F. Evans, N. E. Crook, Insect viruses and pest management, John Wiley & Sons, 1998.

[2] J. P. Burden, R. D. Possee, S. M. Sait, L. A. King, R. S. Hails, Phenotypic and genotypic characterisation of persistent baculovirus infections in populations of the cabbage moth (*Mamestra brassicae*) within the british isles, Arch. Virol. 151 (2006) 635–649.

[3] D. J. Hodgson, A. J. Vanbergen, A. D. Watt, R. S. Hails, J. S. Cory, Phenotypic variation between naturally co-existing genotypes of a lepidopteran baculovirus, Evol. Ecol. Res. 3 (2001) 687–701.

[4] M. D. Ayres, S. C. Howard, J. Kuzio, M. Lopez-Ferber, R. D. Possee, The complete DNA sequence of *Autographa californica* nuclear polyhedrosis virus, Virology 202 (1994) 586–605.

[5] W. F. J. Ijkel, E. A. van Strien, J. G. M. Heldens, R. Broer, D. Zuidema, R. W. Goldbach, J. M. Vlak, Sequence and organisation of the *Spodoptera exigua* multicapsid nucleoployhedrovirus genome, J. Gen. Virol. 80 (1999) 3289–3304.

[6] L. A. King, R. D. Possee, The Baculovirus Expression System; A Laboratory Guide, Chapman & Hall, 1992.

[7] M. Aitken, D. Anderson, B. Francis, J. Hinde, Statistical Modelling in GLIM, Oxford Statistical Science Series 4, Oxford University Press, Oxford, 1989.

Table S1: Fitted parameter values for the infection model using the method outlined in Section 3.2 with the r_0 prescribed by fitting it to the first 7 census points of the control data. See Table 1 in the main manuscript for a comparison.

Parameter	*Ac*NPV	*Paft*NPV	*Mb*NPV	*Se*NPV
Initial Host Mass (g), H_0	4.437×10^{-3}	3.512×10^{-3}	5.5512×10^{-3}	3.763×10^{-3}
Virus Dose (g), V_0	1.25×10^{-9}	4.56×10^{-9}	9.72×10^{-9}	5.19×10^{-10}
Max. Host Growth Rate (h^{-1}), r_0	3.642×10^{-2}	3.642×10^{-2}	3.642×10^{-2}	3.642×10^{-2}
Zero Infection Virus Proportion, p	2.439×10^{-1}	4.058×10^{-2}	2.726×10^{-2}	1.709×10^{-1}
Max. Infection Rate ($g^{-1}h^{-1}$), β_0	19.859	18.130	6.881	16.354
Host Growth Reduction Rate (h^{-1}), a	1.116	26.775	37.104	1.281

(a)

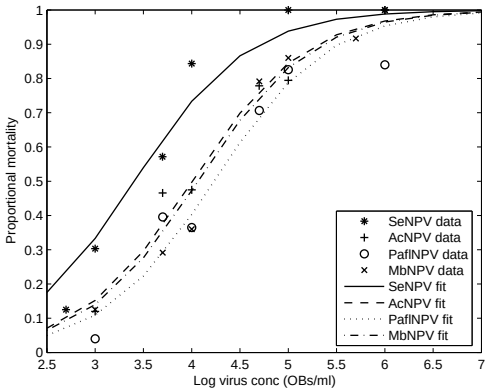

(b)

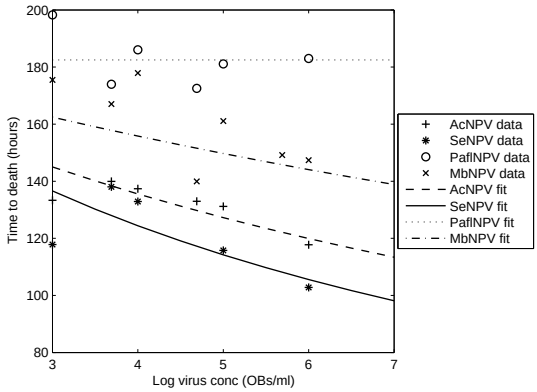

Figure S1: In (a) dose-mortality curves for *Ac*NPV, *Mb*NPV, *Pafl*NPV and *Se*NPV. The lines show the fitted values for *Ac*NPV and *Mb*NPV (logit $= -6.948 + 1.725 \times$ log(virus conc)), *Pafl*NPV (logit $= -7.2812 + 1.725 \times \log$(virus conc)) and *Se*NPV (logit $= -5.802 + 1.725 \times \log$(virus conc)) and proportional mortality is given by $p = 1/(1+(1/e^{\text{logit}}))$. In (b) mean time to death vs dose curves for *Ac*NPV, *Mb*NPV, *Pafl*NPV and *Se*NPV. The lines show the fitted values for *Ac*NPV (time to death $= 1/(0.005454 + 0.0004807 \times \log$ dose)), *Mb*NPV (time to death $= 1/(0.00537152 + 0.0002615 \times \log$ dose)), *Pafl*NPV (time to death $=$ 182.48) and *Se*NPV (time to death $= 1/(0.0051692 + 0.0007172 \times \log$ dose)). The analysis carried-out was inverse transformed with normal errors.

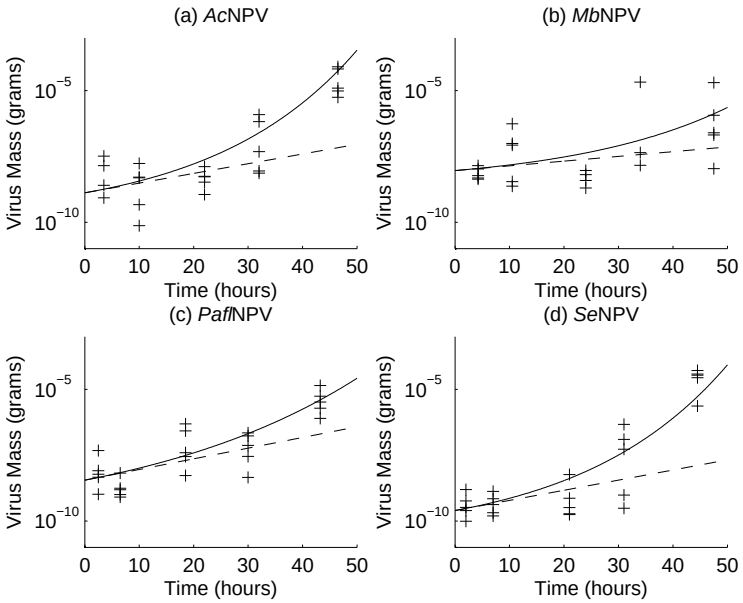

Figure S2: Comparisons of the two approximations for the initial growth of virus. Solid lines denote the double exponential approximation function (B.3); dashed lines denote the exponential approximation function (1). All parameters used are taken from the full ODE model for each virus strain.

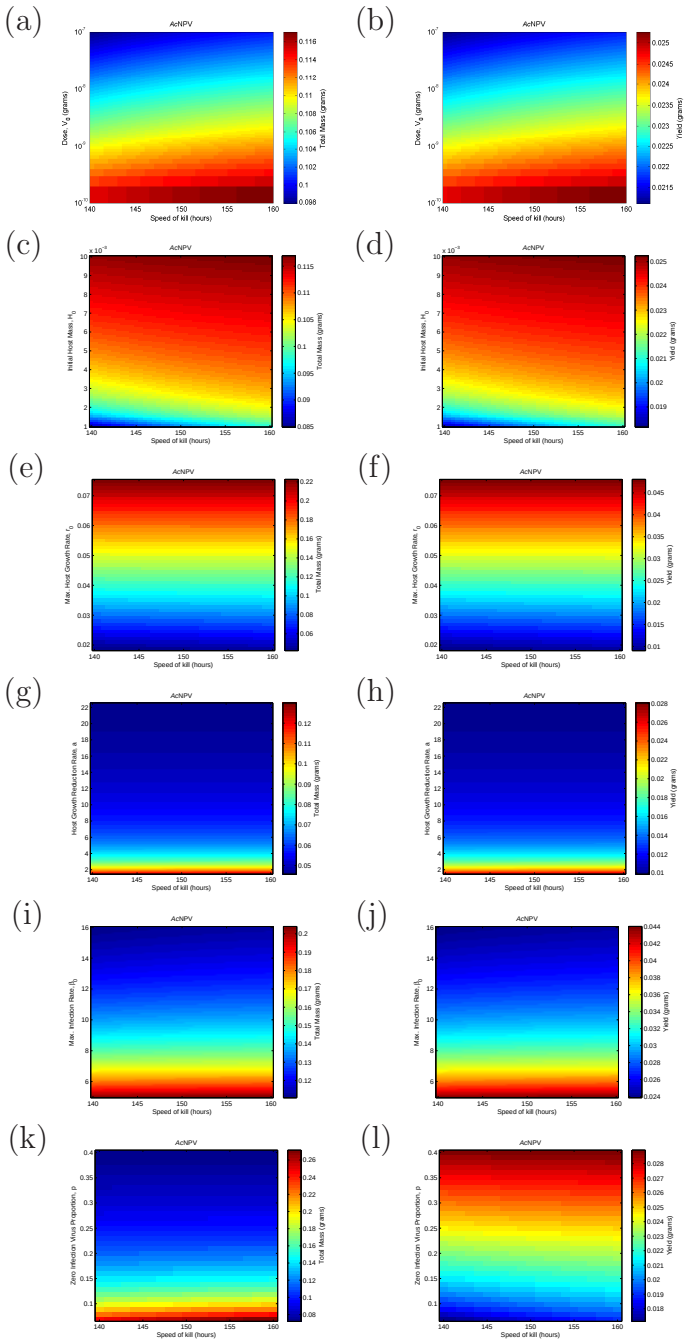

Figure S3: Quantifying the effects of the speed of kill on host mass and yield of virus for *Ac*NPV. Here we run simulations of Model (1) using the parameters in Table 1 for *Ac*NPV. We have plotted the total host mass (left hand column) and viral yield (right hand column) for all 6 parameters (rows). The colours indicate the masses for each parameter and speed of kill combination.

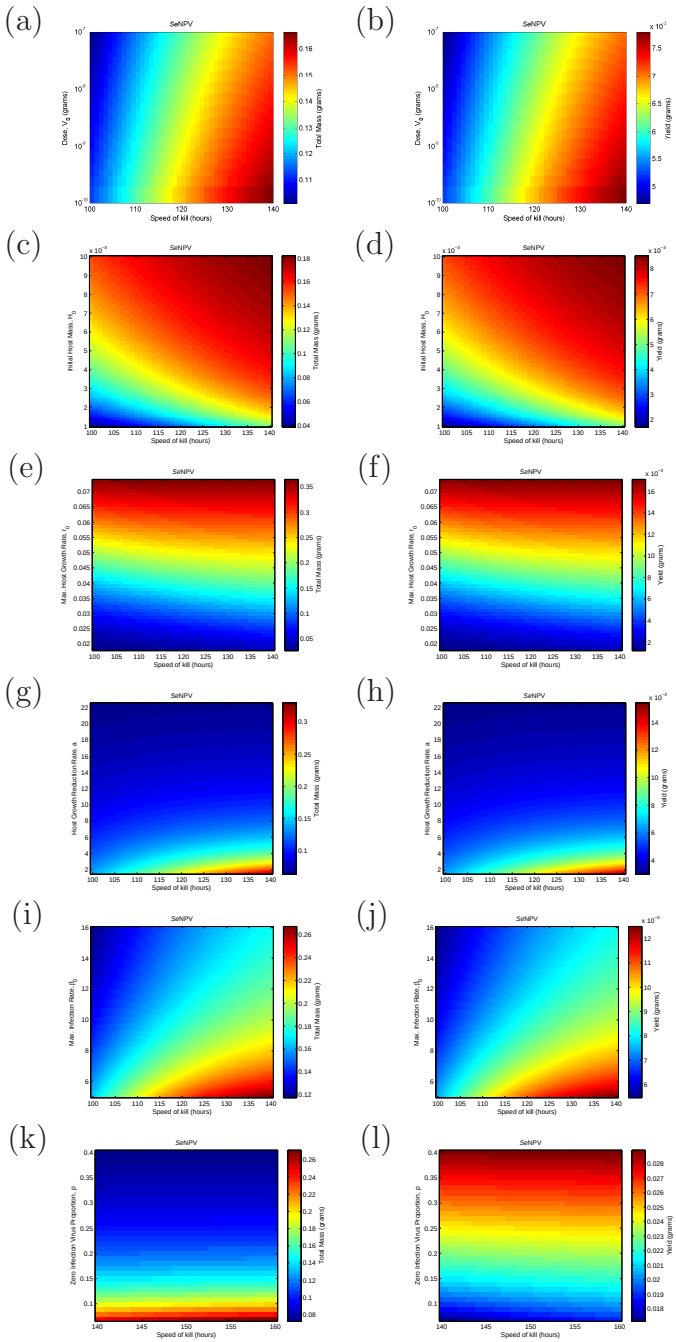

Figure S4: Quantifying the effects of the speed of kill on host mass and yield of virus for *Se*NPV. Here we run simulations of Model (1) using the parameters in Table 1 for *Se*NPV. We have plotted the total host mass (left hand column) and viral yield (right hand column) for all 6 parameters (rows). The colours indicate the masses for each parameter and speed of kill combination.